Biomacromolecules

Article

Cite This: Biomacromolecules 2019, 20, 3385−3391

pubs.acs.org/Biomac

Tailoring Biomimetic Phosphorylcholine-Containing Block Copolymers as Membrane-Targeting Cellular Rescue Agents

Jia-Yu Wang,[†] Wei Chen,[‡,§] Michihiro Nagao,[∥,⊥] Phullara Shelat,[#] Brenton A. G. Hammer,[⊗] Gregory T. Tietjen,[¶] Kathleen D. Cao,[†] J. Michael Henderson,[†] Lilin He,[☆] Binhua Lin,[▽] Bulent Akgun,[∥,◆,⬢] Mati Meron,[▽] Shuo Qian,[☆] Sarah Ward,[⊗] Jeremy D. Marks,[*,#] Todd Emrick,[*,⊗] and Ka Yee C. Lee[*,†]

[†]Department of Chemistry, Institute for Biophysical Dynamics, James Franck Institute, The University of Chicago, Chicago, Illinois 60637, United States

[‡]Center for Molecular Engineering and Materials Science Division, Argonne National Laboratory, Lemont, Illinois 60439, United States

[§]Pritzker School of Molecular Engineering, The University of Chicago, Chicago, Illinois 60637, United States

[∥]NIST Center for Neutron Research, National Institute of Standards and Technology, Gaithersburg, Maryland 20899, United States

[⊥]Center for Exploration of Energy and Matter, Indiana University, Bloomington, Indiana 47408, United States

[#]Department of Pediatrics, The University of Chicago, Chicago, Illinois 60637, United States

[⊗]Department of Polymer Science and Engineering, University of Massachusetts, Amherst, Massachusetts 01003, United States

[¶]Program in the Biophysical Sciences, Institute for Biophysical Dynamics, The University of Chicago, Chicago, Illinois 60637, United States

[☆]Neutron Scattering Division, Oak Ridge National Laboratory, Oak Ridge, Tennessee 37831, United States

[▽]CARS, The University of Chicago, Chicago, Illinois 60637, United States

[◆]Department of Materials Science and Engineering, University of Maryland, College Park, Maryland 20742, United States

[⬢]Department of Chemistry, Bogazici University, Bebek, Istanbul 34342, Turkey

Supporting Information

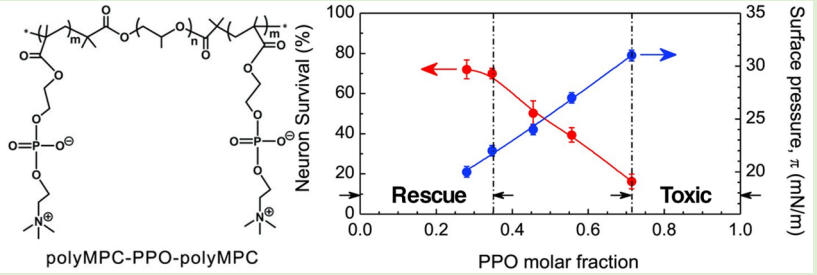

ABSTRACT: Some synthetic polymers can block cell death when applied following an injury that would otherwise kill the cell. This cellular rescue occurs through interactions of the polymers with cell membranes. However, general principles for designing synthetic polymers to ensure strong, but nondisruptive, cell membrane targeting are not fully elucidated. Here, we tailored biomimetic phosphorylcholine-containing block copolymers to interact with cell membranes and determined their efficacy in blocking neuronal death following oxygen-glucose deprivation. By adjusting the hydrophilicity and membrane affinity of poly(2-methacryloyloxyethyl phosphorylcholine) (polyMPC)-based triblock copolymers, the surface active regime in which the copolymers function effectively as membrane-targeting cellular rescue agents was determined. We identified nonintrusive interactions between the polymer and the cell membrane that alter the collective dynamics of the membrane by inducing rigidification without disrupting lipid packing or membrane thickness. In general, our results open new avenues for biological applications of polyMPC-based polymers and provide an approach to designing membrane-targeting agents to block cell death after injury.

INTRODUCTION

Cell membrane dysfunction resulting from loss of lipid bilayer structural integrity is an important pathway toward cell injury and death.[1] Loss of membrane integrity follows cellular

Received: May 6, 2019
Revised: July 16, 2019
Published: August 19, 2019

DOI: 10.1021/acs.biomac.9b00621
Biomacromolecules 2019, 20, 3385−3391

stresses, such as heat, pressure, radiation, electropermeabilization, mechanical shear, and oxidation.[2] Oxidative stress and membrane lipid peroxidation are central mechanisms of numerous disease states leading to cell death, such as neurodegeneration following hypoxia-ischemia (defined as an injurious diminished supply of oxygen and blood to the brain).[3] Although the precise mechanisms of interactions have not been delineated, polymers containing hydrophilic poly(ethylene oxide) (PEO), and triblock copolymers consisting of PEO and the more hydrophobic poly(propylene oxide) (PPO), have been shown to block cell death when introduced after a variety of stimuli.[2,4−6] However, a fundamental understanding of how these polymers interact with cell membranes is lacking, precluding determination of the central molecular parameters required for optimal materials design.

Previous studies of polymer−membrane interactions demonstrated that PEO-PPO-PEO triblock copolymers effectively protect liposomes from oxidative and osmotic stress, with the relative ratio between PEO and PPO determining the nature of polymer−membrane interactions, and the hydrophobicity of the copolymer determining the ability of the polymer to insert and anchor to the membrane.[7,8] In particular, PEO-PPO-PEO triblock copolymers with a high degree of hydrophobicity act as membrane permeabilizers.[9] While PEO homopolymers protect membranes from damage, PEO-PPO-PEO triblock copolymers function at orders of magnitude lower concentration. The hydrophobic PPO block likely enhances the residence time of the polymer at the membrane surface, promoting efficacy even at low concentration. Furthermore, altering the relative size of the hydrophilic and hydrophobic moieties allows advantageous tuning of the hydrophilic−lipophilic balance (HLB). These observations led us to hypothesize that an effective membrane-targeting cellular rescue polymer requires two key features: (i) a major hydrophilic component to promote adsorption at the membrane surface without penetration into the bilayer and (ii) a minor hydrophobic component to provide nondisruptive anchoring in the membrane. In this study, we describe the adjustment of polymer HLB for the purpose of identifying the roles of these components in determining polymer−membrane interactions and optimizing them to maximize neuronal rescue following injury.

EXPERIMENTAL SECTION

Synthesis of polyMPC-PPO-polyMPC. The PPO macroinitiator, CuBr, 2,2′-bipyridine, and methacryloyloxyethyl phosphorylcholine (MPC) were dissolved in anhydrous methanol in a round-bottom flask that was cooled in an ice−water bath (specific details in SI). The polymerization was conducted under a nitrogen atmosphere at room temperature for 2.5 h and the polymer was isolated by precipitation in anhydrous tetrahydrofuran (THF), then purified by passage through a short plug of silica gel.

Preparation of Lipid Monolayers. Lipid monolayers were prepared on a Langmuir trough by dropwise addition of a chloroform solution of polymer at the air/water interface, then left for 15 min to allow solvent evaporation. Compression at a linear speed of 0.1 mm/s was performed until the system reached its target surface pressure. The surface pressure was measured by a Wilhelmy plate-type transducer with a filter-paper plate.

Preparation of Large Unilamellar Vesicles (LUVs). Large unilamellar vesicles (LUVs) were prepared via the freeze−thaw extrusion method (see SI for details).

Postnatal Hippocampal Neuronal Cultures. Hippocampal neurons were prepared and maintained as described previously.[23]

Oxygen Glucose Deprivation (OGD). OGD experiments were performed deoxygenated glucose-free bicarbonate-buffered saline containing 95 mmol/L NaCl, 5.3 mmol/L KCl, 1.3 mmol/L NaH_2PO_4, 1.3 mmol/L $MgSO_4$, 24 mmol/L $NaHCO_3$, and 2.4 mmol/L $CaCl_2$. To prepare saline for OGD experiments, the bicarbonate buffer was incubated in a hypoxia workstation, where O_2 and CO_2 levels were continuously maintained at 1% and 5%, respectively. For control experiments without OGD challenge, the bicarbonate buffer with 25 mmol/L glucose and 1 mmol/L succinate was incubated in a conventional humidified 5% CO_2 incubator. Both saline solutions were incubated for 18 h before transferring cultured neurons to them. The *in vitro* cellular experiments were performed by incubation of neurons either under the OGD condition or in the control saline solution for 45 min. After that, the neurons were transferred back to their original neurobasal medium where polyMPC homopolymer or poly(MPC-PO-MPC) triblock copolymer was introduced to study the potential of these polymers in rescuing injured neurons from hypoxic injury. Before each experiment, dead neurons were removed by incubation in DNase (900 U/mL) for 1 h.

Evaluation of Neuronal Survival. Cell survival was evaluated using the unbiased automated total-live cell assay 48 h after OGD. Briefly, cells stained by both 4′,6-diamidino-2-phenylindole (DAPI) and calcein acetoxymethylester (calcein-AM) were identified as live, whereas neurons stained only by DAPI (blue) were categorized as dead. To evaluate neuronal survival, at least 42 equally distributed fields that contain at least 1300 neurons from at least six coverslips for each condition in each experiment were counted. The statistical analysis was performed by one-way analysis of variance (ANOVA) followed by the Tukey test ($p < 0.05$ were accepted as significant).

Evaluation of Polymer Surface Activity and Constant Surface Pressure Insertion Assay. The surface activity of polyMPC homopolymers and poly(MPC-PO-MPC) triblock copolymers was monitored through their adsorption kinetics at the air−water interface. The quantification of polymer insertion into lipid monolayers was conducted using a constant pressure insertion assay. In general, lipid monolayers were prepared and kept at $\pi = 30$ mN/m, a bilayer equivalent pressure, via a built-in feedback system that adjusts the surface area. PolyMPC or poly(MPC-PO-MPC) was injected into the subphase. If the injected polymer interacts with lipid membranes through insertion, π would increase. To keep π constant, A must increase. Thus, the relative area change, $\Delta A/A_0$, reflects the degree of polymer insertion into the lipid film.

Neutron Spin Echo (NSE). NSE measurements were performed using the NG5-NSE spectrometer at the Center for Neutron Research of National Institute of Standards and Technology (NCNR-NIST). The 8 Å incident neutron beam was selected with wavelength resolution of approximately 20%. A set of polarizers and analyzers was employed to analyze the neutron polarization. The Larmor precession of neutron spin in a magnetic field was used as a precise measure of energy transfer between the neutrons and the sample. The covered ranges of momentum transfer, q, and time, t, were $0.04\ Å^{-1} < q < 0.13\ Å^{-1}$ and $0.5\ ns \leq t \leq 40\ ns$, respectively.

Small-Angle Neutron Scattering (SANS). SANS experiments were conducted on the NG7-SANS instrument at NCNR-NIST and the CG-3 Bio-SANS instrument of the High Flux Isotope Reactor at Oak Ridge National Laboratory (ORNL). The incident neutron wavelength, λ, at NIST was selected to be 6 Å for 1 and 4 m configurations and 8.9 Å for 15.3 m configuration, with a wavelength resolution of approximately 11%. λ at ORNL was selected to be 6 Å for 1.1 and 6.8 m configurations and 12 Å for 15.3 m configuration, with a wavelength resolution of approximately 15%. With these configurations, q was measured from $0.001\ Å^{-1}$ to $0.557\ Å^{-1}$ at NIST and $0.002\ Å^{-1}$ to $0.717\ Å^{-1}$ at ORNL.

Grazing Incidence X-ray Diffraction (GIXD). GIXD experiments were performed at the Advanced Photon Source (APS) of Argonne National Laboratory using ChemMatCARS in Sector 15-ID-C.[24] The wavelength of the X-ray beam was 1.24 Å, corresponding to an energy of 10 keV.

DOI: 10.1021/acs.biomac.9b00621
Biomacromolecules 2019, 20, 3385−3391

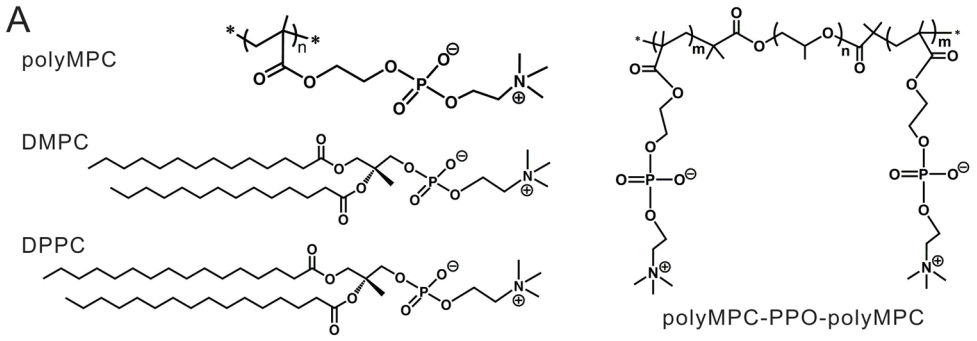

Sample	description	M_nX10^3	M_w/M_n	# of MPC units	# of PO units	PPO fraction	π_{max} (mN/m)	CMC (μmol/L)
HP_9K[30]	polyMPC homopolymer	9	1.25	30	-	-	0	-
HP_13K[43]	polyMPC homopolymer	13	1.3	43	-	-	0	-
HP_27K[90]	polyMPC homopolymer	27	1.3	90	-	-	0	-
BCP_6.5K[14]	polyMPC-PPO-polyMPC	6.5	1.3	14	35	0.714	31.5±0.8	15
BCP_10.5K[28]	polyMPC-PPO-polyMPC	10.5	1.3	28	35	0.556	27.3±0.5	30
BCP_15K[42]	polyMPC-PPO-polyMPC	15	1.25	42	35	0.455	25.8±0.7	35
BCP_22K[66]	polyMPC-PPO-polyMPC	22	1.3	66	35	0.374	23.8±0.4	40
BCP_29K[90]	polyMPC-PPO-polyMPC	29	1.45	90	35	0.280	20.1±0.2	>50

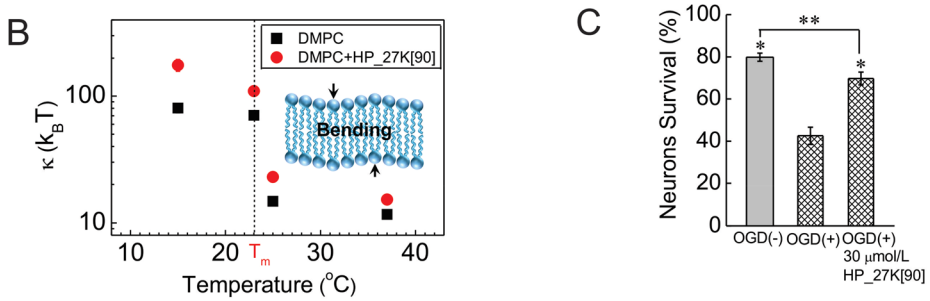

Figure 1. Effects of polyMPC homopolymer on model membranes and injured neurons. (A) Molecular structure of polyMPC, polyMPC-PPO-polyMPC, DMPC and DPPC lipids. (B) The bending modulus, κ, as a function of temperature for (■) DMPC and (red ●) DMPC membranes in the presence of 200 μmol/L HP_27K[90] in a water medium. Inset: A sketch of a lipid bilayer. (C) Quantification of the effects of polymers on cultured embryonic rat hippocampal neuron survival following OGD at 37 °C in the presence of homopolymer HP_27K[90] at a polymer concentration of 30 μmol/L. *p < 0.05 as compared to OGD (+); ** p < 0.05 as compared to OGD (−). Error bars represent ±1 standard deviation in the present paper.

■ RESULTS AND DISCUSSION

To test our hypothesis, we designed polymers that replace the PEO blocks of PEO-PPO-PEO triblock copolymers with poly(2-methacryloyloxyethyl phosphorylcholine) (polyMPC) blocks. PolyMPC is a zwitterionic polymer composed of a methacrylate backbone and pendent phosphorylcholine (PC) moieties;[10] it exhibits exceptional hydrophilicity, is biodegradable and blood-compatible, and resists protein adsorption when grafted to surfaces.[11,12] PolyMPC homopolymers were synthesized by atom transfer radical polymerization[13] (ATRP) (Figure 1A, top left; sample names starting with HP) and their surface activity was characterized at the water−air interface. Unlike PEO homopolymers, which are surface-active[14] (Gibbs adsorption surface pressure of ≈10 mN/m[14]), polyMPC homopolymers exhibited no surface activity (Figure S1), indicating that polyMPC partitions into water and further suggesting a potential lack of strong interactions with membranes.

To determine the extent of interactions between polyMPC and lipid membranes, model membrane systems were combined with scattering techniques to characterize lipid packing, membrane thickness, and the collective dynamics. We first modeled the outer leaflet of a lipid membrane using monolayers of 1,2-dipalmitoyl-*sn*-glycero-3-phosphocholine (DPPC). GIXD probed in-plane ordering, while X-ray (XR) and neutron reflectivity (NR) characterized the out-of-plane electron density distribution in the presence and absence of the 90-mer polyMPC homopolymer HP_27K[90] (27 kDa, Figure 1A). Interestingly, the presence of HP_27K[90] induced no differences in the GIXD, XR, and NR profiles (Figures S2, S3), indicating that polyMPC does not alter lipid packing or membrane thickness. Next, large unilamellar vesicles (LUVs) of 1,2-dimyristoyl-*sn*-glycero-3-phosphocholine (DMPC) were employed as a simple model of fluid membranes. Small angle neutron scattering (SANS) studies showed HP_27K[90] to have no effect on membrane static structure, regardless of membrane curvature or lipid packing density (Figure S4). In contrast, neutron spin echo (NSE) measurements of DMPC LUVs in the presence and absence of HP_27K[90] demonstrated that polyMPC alters the collective dynamics of the membrane. Unlike GIXD, XR, NR, and SANS, which directly probe the membrane structure, NSE yields information on membrane fluctuations from which one can determine how the presence of the polymer can affect membrane undulations. For pure DMPC LUVs, the bending modulus (κ) was 12−15 k_BT above the DMPC gel−liquid crystal transition temperature

DOI: 10.1021/acs.biomac.9b00621
Biomacromolecules 2019, 20, 3385−3391

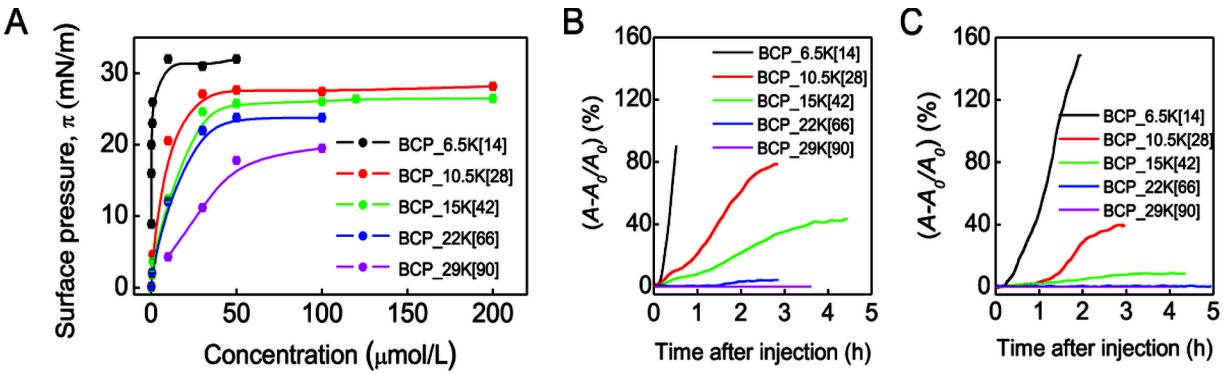

Figure 2. Interfacial activities of polyMPC-PPO-polyMPC. (A) Gibbs adsorption isotherms at the air/water interface and 25 °C. (B,C) Change of area per lipid molecule after insertion of polyMPC-PPO-polyMPC into a (B) DMPC monolayer and (C) DPPC monolayer at π = 30 mN/m and 25 °C. The polymer concentration in the water subphase was 50 μmol/L. Note: $(A - A_0)/A_0$ of DMPC and DPPC for BCP_6.5K[14] does not represent equilibrium values as the barrier had reached its physical limitation. The observed difference of $(A - A_0)/A_0$ for the two monolayers is due to their distinctive A_0 at 30 mN/m, where A_{0_DMPC} is 56 Å^2/mol and A_{0_DPPC} is 45 Å^2/mol.

(T_m) of 23 °C, and 70 k_BT below T_m. The presence of HP_27K[90], however, increased κ by ~30% above T_m, ~50% near T_m, and >100% below T_m (Figures 1B and S5), demonstrating that the homopolymer increases membrane rigidity. This polymer-induced membrane rigidification in the absence of any detectable structural changes indicates weak interactions between the polymer and the lipid membrane, possibly driven by dipole−dipole attraction of the PC zwitterions.[15] Collectively, the XR and NR measurements demonstrate that while polyMPC is not surface-active, it nonetheless alters lipid membranes through weak, non-disruptive interactions. The weak absorption of polyMPC homopolymers on lipid bilayers was further confirmed via surface force apparatus experiments (see Figure S6).

Having found the polyMPC homopolymer to interact weakly with model membranes, the potential for these polymers to assist in rescuing injured neurons from severe injury was examined. Using cultured rat embryonic hippocampal neurons, oxygen glucose deprivation (OGD) was employed as an *in vitro* model of brain hypoxia-ischemia[6] that results in widespread neuronal apoptosis within 48 h of injury. Neurons on coverslips were exposed to 45 min OGD, or to otherwise identical, control solutions containing glucose at ambient oxygen tension. After OGD or control exposure, the coverslips were returned to their culture dishes with the original, glucose-containing media, half of which also contained HP_27K[90] (30 μM), then all the dishes were returned to the incubator. After 48 h, unbiased counts of living and dead neurons were made with high-content imaging, counting ~1300 total neurons per coverslip. Measurements recorded 48 h after exposure to the control solutions showed a mean neuronal survival of 79.8 ± 2% (SEM), while OGD significantly decreased mean neuronal survival to 42.6 ± 4%, (p < 0.001). Notably, survival of OGD-treated neurons incubated in the presence of HP_27K[90] (69.7 ± 3%, Figure 1C) increased markedly compared to OGD alone (p < 0.001), suggesting that simply the presence of polyMPC homopolymer alters mechanisms of apoptotic neuronal death.

Examined next was whether adding a hydrophobic block to polyMPC would alter its behavior with neuronal cells relative to polyMPC alone. Starting from a PPO "macroinitiator", growth of the polyMPC blocks afforded polyMPC-PPO-polyMPC triblock copolymers. PPO block sizes were selected to be similar to those of Poloxamer 188 (PEO_{80}-PPO_{27}-PEO_{80}), a copolymer with known affinity for cell membranes.[4,16−18] As a first test-case, polyMPC$_{45}$-PPO$_{35}$-polyMPC$_{45}$, BCP_29K[90], (29 kDa, see Figure 1A for nomenclature) was prepared, an ABA triblock copolymer with a PPO mole fraction (f_{PPO}) of 0.28. Remarkably, incubation of hippocampal neurons in the presence of BCP_29K[90] (30 μM) following OGD completely rescued neurons from OGD-induced death at 48 h (Figure 1C). Moreover, survival following BCP_29K[90] was significantly (P = 0.0002) greater than survival following the polyMPC homopolymer HP_27K[90]. These data indicate that the presence of a central hydrophobic component markedly increases the efficacy of polyMPC-mediated neuronal rescue.

The impact of the HLB of polyMPC-PPO-polyMPC copolymers on their association with lipid membranes was then evaluated. Four additional polyMPC-PPO-polyMPC triblock copolymers were synthesized, keeping the 35-mer PPO block constant and varying the polyMPC blocks from 14 (f_{PPO} = 0.71) to 66 (f_{PPO} = 0.37) monomer units. With greater polyMPC molecular weight, the copolymers became increasingly hydrophilic and their surface activity declined (Figure 1A). In accord with these findings, the critical micelle concentration (CMC), determined from the surface activity of the polymer at the air−water interface,[19] also increased (Figures 1A and 2A).

We next examined, using a constant surface pressure insertion assay, whether the polyMPC-containing triblock copolymers inserted into lipid membranes or simply associated with the membrane surface. Since polymer insertion into such a membrane is affected by membrane fluidity,[20] two different lipid monolayers were studied: the more fluidic (less ordered) DMPC and the less fluidic (more ordered) DPPC (Figure S7A). BCP_6.5K[14], the most hydrophobic of the triblock copolymers, intercalated into both lipid films rapidly and extensively (Figure 2B,C, Figure S7). In contrast, polymers of intermediate hydrophobicity, BCP_10.5K[28] and BCP_15K[42], preferentially penetrated into the DMPC monolayer (Figure 2B) relative to the more ordered DPPC monolayer (Figure 2C), demonstrating the importance of membrane fluidity in governing polymer−membrane interactions. However, the most hydrophilic copolymers, BCP_22K[66] and BCP_29K[90], failed to penetrate into either lipid film (Figure 2B,C), since the longer polyMPC blocks dominate their solution and interfacial behavior. These

DOI: 10.1021/acs.biomac.9b00621
Biomacromolecules 2019, 20, 3385−3391

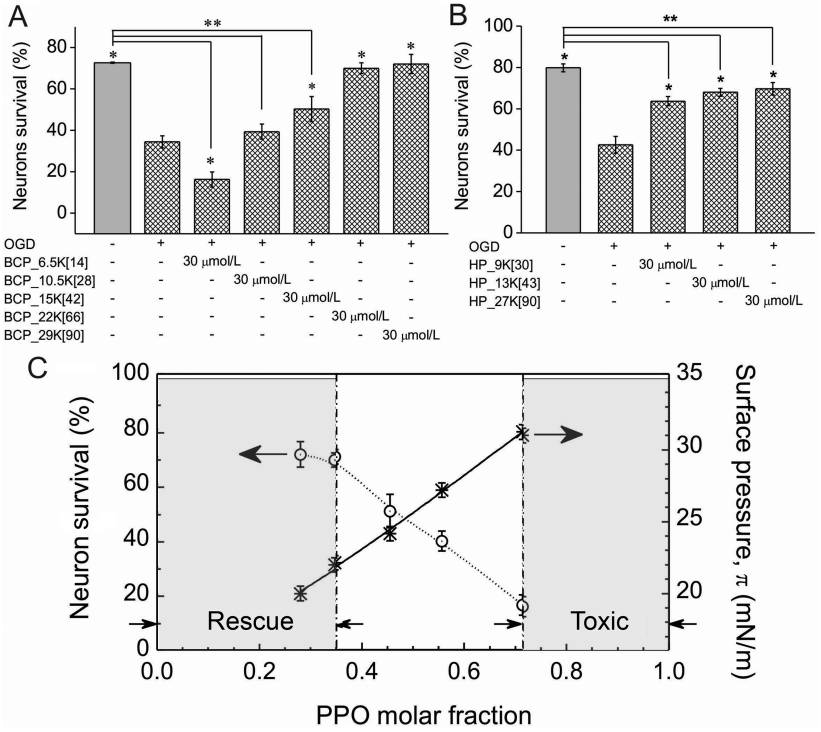

Figure 3. Effects of polyMPC-PPO-polyMPC triblock copolymers and polyMPC homopolymers on neuronal survival. (A) Quantification of the effects of polyMPC-PPO-polyMPC on cultured embryonic rat hippocampal neuron survival following OGD at 37 °C. (B) Quantification of the effects of molecular weight of polyMPC homopolymer on cultured embryonic rat hippocampal neuron survival following OGD at 37 °C. * $p < 0.05$ as compared to OGD (+); ** $p < 0.05$ as compared to OGD (−). (C) The correlation among the Gibbs adsorption surface pressure, π, neuronal survival, and the molar fraction of PPO for polyMPC-PPO-polyMPC at a polymer concentration of 30 μmol/L. PolyMPC-PPO-polyMPC with $f_{PPO} < 0.35$ is expected to be a membrane-targeting cellular rescue agent; polyMPC-PPO-polyMPC with $f_{PPO} > 0.71$ is expected to be toxic to neurons.

experiments demonstrate that the degree of copolymer insertion scales with its wetting characteristics, with the most hydrophilic samples resisting insertion into the lipid films.

Similar OGD experiments were performed with these zwitterionic triblock copolymers to elucidate their behavior in the presence of neuronal cells, finding that the degree of membrane insertion of the five copolymers correlated inversely with their efficacy in rescuing injured neurons. As with BCP_29K[90], the noninserting BCP_22K[66] also fully protected neurons from death following OGD (Figures 3A and S7). BCP_15K[42], with only minor membrane insertion capability, provided a small but significant level of neuronal rescue following OGD (Figure 3A). BCP_6.5K, exhibiting the greatest membrane insertion, failed to rescue neurons following OGD. In fact, this membrane-inserting copolymer was measurably toxic and increased neuronal death over the level seen following OGD (Figure 3A). This decline in neuronal rescue capacity is likely due to membrane disruption associated with a greater degree of insertion for this more hydrophobic polymer with less polyMPC content.

As the most effective copolymer examined had the highest molecular weight, we used a series of polyMPC homopolymers (Figure 1A) to test how polymer molecular weight, or f_{PPO}, impacted neuronal rescue efficacy. The lower molecular weight homopolymers (HP_9[30], HP_13[43]) exhibited similarly modest rescue capabilities (Figure 3B), not significantly different from HP_27[90]. These data suggest that the improved neuronal survival seen in poly(MPC-PO-MPC) is due to the decrease in f_{PPO}, or the relative hydrophobicity of the copolymer, rather than the overall size of the individual polymer blocks. An overlay of surface activities of the copolymers with their neuronal rescue capability (Figure 3C) indicates that poly(MPC-PO-MPC) triblock copolymers with surface tension π-values <21 mN/m are potentially effective membrane-targeting cellular rescue agents, and those with π greater than 31 mN/m are cytotoxic. Accordingly, our findings demonstrate that polymer synthesis can be utilized effectively to achieve the desired surface activity and effect either cell toxicity or cell rescue.

Further insight into the biophysical mechanisms of neuronal rescue/neurotoxicity of poly(MPC-PO-MPC) triblock copolymers was gained by examining the effects of hydrophilic BCP_22K[66] and hydrophobic BCP_6.5K[14] on lipid packing, as the lateral organization of lipid molecules influences membrane biology.[21] Because a DPPC monolayer at 30 mN/m forms ordered phases that can be detected easily by GIXD, this was selected as a model system. GIXD showed two distinct Bragg peaks in each monolayer/homopolymer combination, demonstrating distorted hexagonal packing of the lipid tails. Similar to homopolymer HP_27K[90], the Bragg peaks resulting from a pure DPPC film (Figure 4A, top) and that with BCP_22K[66] present (Figure 4A, middle), have almost identical peak positions, with their corresponding Bragg rod profiles sharing very similar features (Figure S9). These results indicate that BCP_22K[66] has little influence on DPPC packing. Despite these hydrophilic polymers having no discernible effects on lipid packing, neutron spin echo results (Figure 1B) showed that these homopolymers are nonetheless capable of altering membrane rigidity, a property crucial for regulation of membrane protein function.[22] The ability of these

DOI: 10.1021/acs.biomac.9b00621
Biomacromolecules 2019, 20, 3385−3391

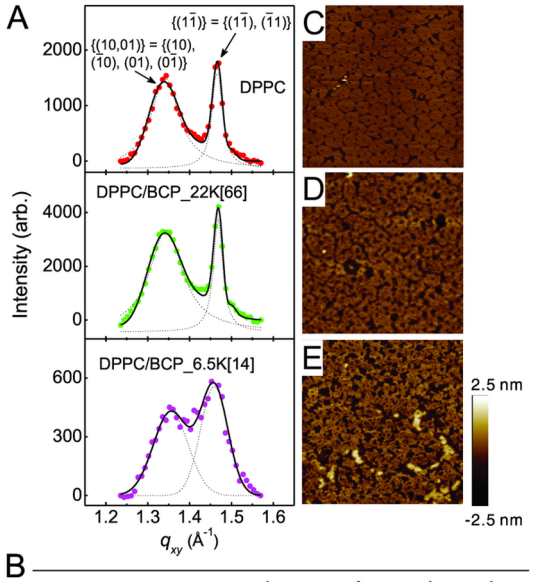

B

Sample	*a*, *b* (Å)	γ (°)	$A_{unit\ cell}$ (Å^2)	L_{10} (Å)	L_{11} (Å)
DPPC	5.13	113	24.0	68	232
DPPC+BCP_22K[66]	5.11	113	24.0	57	243
DPPC+BCP_6.5K[14]	5.10	115	23.6	68	89

Figure 4. Effects of BCP_22K[66] and BCP_6.5K[14] on packing of lipids. (A) Bragg peaks from GIXD on a pure DPPC monolayer (top panel), and a DPPC monolayer in the presence of BCP_22K[66] (middle panel) or BCP_6.5K[14] (bottom panel) in a water subphase at π = 30 mN/m and T = 23 °C. The two Bragg peaks observed from the DPPC monolayers indicate distorted-hexagonal packing of the lipid tails in a 2-D unit cell and the corresponding Miller indices are indicated for each peak. (B) Parameters obtained from the GIXD profiles. *a*, *b*, and γ are the axes of a unit cell and the angle across from the *a* and *b* axis, respectively; $A_{unit\ cell}$ is the area of a unit cell; L_{10} and L_{11} are coherence length in the direction of {(10, 01)} and {11̄}, respectively. The GIXD measurements were taken at A_{DPPC} = 47.3 Å^2, $A_{DPPC+BCP\_22K[66]}$ = 47.3 Å^2 and $A_{DPPC+BCP\_6.5K[14]}$ = 61 Å^2. (C–E) AFM height images (2 μm × 2 μm) of the DPPC monolayer (C), DPPC monolayer in the presence of BCP_22K[66] (D), or BCP_6.5K[14] (E) on a water subphase deposited onto a mica substrate at π = 30 mN/m and T = 25 °C. The two different domains observed in the DPPC monolayers are the liquid condensed (LC) phase (bright pinwheel-like shape) that gives rise to Bragg diffraction in GIXD, and the liquid-expanded (LE) phase (darker noncontinuous area) within which the hydrocarbon chains are highly disordered.

copolymers to affect the mechanical properties of the membrane thus plays an important role in neuronal rescue.

In contrast, GIXD revealed BCP_6.5K to markedly reduce correlation length, L_{11}, from 232 to 89 Å (Figure 4B). As correlation length represents the average distance over which crystallinity extends, these results indicated that BCP_6.5K disrupted the long-range order of DPPC lipids and induced membrane defects. These membrane defects may arise from the mismatch in size and hydrophobicity between PPO and the hydrocarbon lipid tails. Interestingly, insertion of BCP_6.5K also slightly increased the packing of DPPC molecules remaining in the ordered phase, as indicated by the closer separation of the two Bragg peaks (Figure 4A, bottom). The GIXD data demonstrate that polymer insertion reduced both the tilt angle and the area of the lipid tail: the tilt angle θ of the tail dropped from 30° to 28.3° and the area per tail declined from 24.0 to 23.6 Å^2, representing a 1.7% increase in packing density (Figure 4B and Figure S9). Despite small, local enhancement in lipid ordering, membrane defect formation resulting from polymer insertion appears to dominate, which compromises the structural integrity of the membrane. This finding was corroborated by atomic force microscopy (AFM) and leakage measurements (Figure 4C–E and Figure S10). Our data thus point to membrane disruption induced by polymer insertion as the cause of cytotoxicity of BCP_6.5K[14].

CONCLUSIONS

Physicochemical characterization of polyMPC block copolymers revealed the mechanism by which this class of polymers interacts with lipid membranes, and cell survival studies identified the surface activity regime in which polyMPC-PPO-polyMPC triblock copolymers function effectively as membrane-targeting cellular rescue agents. The results presented provide general guidelines for rational selection and synthesis of new biomaterials that effectively function in cellular protection and rescue events. Furthermore, the discovery of the cytoprotective effect of polyMPC-based triblock copolymers provides a new platform for innovative biotechnology and medicine using this important class of medically relevant polymer zwitterions.

ASSOCIATED CONTENT

Supporting Information

The Supporting Information is available free of charge on the ACS Publications website at DOI: 10.1021/acs.biomac.9b00621.

Description of materials, methods and instruments; ^{1}H NMR spectra and gel permeation chromatography data, GIXD, XR, NR, SANS and NSE data, model fits, and associated fit parameters, pressure–area isotherms fluorescence images (PDF)

AUTHOR INFORMATION

Corresponding Authors

*Ka Yee C Lee. E-mail: kayeelee@uchicago.edu.
*Jeremy D. Marks. E-mail: j-marks1@uchicago.edu.
*Todd Emrick. E-mail: tsemrick@mail.pse.umass.edu.

ORCID

Wei Chen: 0000-0001-8906-4278
Binhua Lin: 0000-0001-5932-4905
Shuo Qian: 0000-0002-4842-828X
Todd Emrick: 0000-0003-0460-1797

Notes

The authors declare no competing financial interest.

ACKNOWLEDGMENTS

We thank Xiangji Chen for providing polyMPC homopolymers, Yun Liu for assistance with SANS measurements, and Paul D. Butler for valuable discussions. J.-Y.W., G.T.T., K.D.C., J.M.H., and K.Y.C.L. acknowledge the support of the NSF (MCB-0920316 and MCB-1413613) and the University of Chicago NSF-MRSEC program (DMR-0820054 and DMR-1420709). W.C. gratefully acknowledges the financial support from the U.S. Department of Energy, Office of Science, Materials Science and Engineering Division. P.S. and J.D.M. acknowledge the support of NIH Health Grants (R01 NS-

DOI: 10.1021/acs.biomac.9b00621
Biomacromolecules 2019, 20, 3385–3391

056313 and T32 HL-094282). B.A.G.H. and T.E. acknowledge funding from the NSF-supported UMass MRSEC on Polymers and the Materials Research Facilities Network (NSF-MRSEC-DMR-0820506). M.N. acknowledges funding from cooperative agreement 70NANB15H259 from NIST, U.S. Department of Commerce. We acknowledge the support of NIST, DOC, in providing the neutron research facilities used in this work. Access to the NG5-NSE was provided by the Center for High Resolution Neutron Scattering, a partnership between the National Institute of Standards and Technology and the National Science Foundation under Agreement No. DMR-1508259. The Bio-SANS instrument used in this study is a resource of the Center for Structural Molecular Biology at ORNL, which is supported by DOE, the Office of Biological and Environmental Research. Bio-SANS is located at ORNL-HFIR, which is sponsored by DOE, the Scientific User Facilities Division, Office of Basic Energy Sciences. ChemMatCARS is principally supported by the NSF/DOE (CHE-0087817). The APS is supported by the DOE, Basic Energy Sciences, and Office of Science (W-31-109-Eng-38). The work also utilized the Materials Research Facilities Network (MRFN-DMR-5-44456) and facilities supported in part by the NSF (DMR-0944772).

REFERENCES

(1) McNeil, P. L.; Steinhardt, R. A. Plasma membrane disruption: repair, prevention, adaptation. *Annu. Rev. Cell Dev. Biol.* **2003**, *19*, 697−731.

(2) Lee, R. C. Cytoprotection by stabilization of cell membranes. *Ann. N. Y. Acad. Sci.* **2002**, *961*, 271−275.

(3) Lee, J. M.; Zipfel, G. J.; Choi, D. W. The changing landscape of ischaemic brain injury mechanisms. *Nature* **1999**, *399*, A7−14.

(4) Yasuda, S.; Townsend, D.; Michele, D. E.; Favre, E. G.; Day, S. M.; Metzger, J. M. Dystrophic heart failure blocked by membrane sealant poloxamer. *Nature* **2005**, *436*, 1025−1029.

(5) Shi, Y.; Kim, S.; Huff, T. B.; Borgens, R. B.; Park, K.; Shi, R.; Cheng, J.-X. Effective repair of traumatically injured spinal cord by nanoscale block copolymer micelles. *Nat. Nanotechnol.* **2010**, *5*, 80−87.

(6) Shelat, P. B.; Plant, L. D.; Wang, J. C.; Lee, E.; Marks, J. D. The membrane-active tri-block copolymer pluronic F-68 profoundly rescues rat hippocampal neurons from oxygen-glucose deprivation-induced death through early inhibition of apoptosis. *J. Neurosci.* **2013**, *33*, 12287−12299.

(7) Wang, J. Y.; Marks, J.; Lee, K. Y. Nature of interactions between PEO-PPO-PEO triblock copolymers and lipid membranes: (I) effect of polymer hydrophobicity on its ability to protect liposomes from peroxidation. *Biomacromolecules* **2012**, *13*, 2616−262.

(8) (a) Cheng, C. Y.; Wang, J. Y.; Kausik, R.; Lee, K. Y.; Han, S. Nature of interactions between PEO-PPO-PEO triblock copolymers and lipid membranes: (II) role of hydration dynamics revealed by dynamic nuclear polarization. *Biomacromolecules* **2012**, *13*, 2624−2633. (b) Maskarinec, S. A.; Hannig, J.; Lee, R. C.; Lee, K. Y. C. DIrect Observation of Poloxamer 188 Insertion into Lipid Monolayers. *Biophys. J.* **2002**, *82*, 1453−1459. (c) Frey, S. L.; Zhang, D.; Carignano, M. A.; Szleifer, I.; Lee, K. Y. C. Effects of Block Copolymer's Architecture on Its Association with Lipid Membranes: Experiments and Simulations. *J. Chem. Phys.* **2007**, *127*, 114904. (d) Wang, J.; Segatori, L.; Biswal, S. L. Probing the Association of Triblock Copolymers with Supported Lipid Membranes Using Microcantilevers. *Soft Matter* **2014**, *10*, 6417−6424. (e) Houang, E. M.; Bates, F. S.; Sham, Y. Y.; Metzger, J. M. All-atom Molecular Dynamic-based Analysis of Membrane-stabilizing Copolymer Interactions with Lipid Bilayers Probed under Constant Surface Tensions. *J. Phys. Chem. B* **2017**, *121*, 10657−10664.

(9) Wang, J. Y.; Chin, J.; Marks, J. D.; Lee, K. Y. Effects of PEO-PPO-PEO triblock copolymers on phospholipid membrane integrity under osmotic stress. *Langmuir* **2010**, *26*, 12953−12961.

(10) Ishihara, K.; Ueda, T.; Nakabayashi, N. Preparation of phospholipid polymers and their Properties as polymer hydrogel membranes. *Polym. J.* **1990**, *22*, 355−360.

(11) Monge, S.; Canniccioni, B.; Graillot, A.; Robin, J. J. Phosphorus-containing polymers: a great opportunity for the biomedical field. *Biomacromolecules* **2011**, *12*, 1973−1982.

(12) Yu, X.; Liu, Z.; Janzen, J.; Chafeeva, I.; Horte, S.; Chen, W.; Kainthan, R. K.; Kizhakkedathu, J. N.; Brooks, D. E. Polyvalent choline phosphate as a universal biomembrane adhesive. *Nat. Mater.* **2012**, *11*, 468−476.

(13) Chen, X.; McRae, S.; Parelkar, S.; Emrick, T. Polymeric phosphorylcholine-camptothecin conjugates prepared by controlled free radical polymerization and click chemistry. *Bioconjugate Chem.* **2009**, *20*, 2331−2341.

(14) Winterhalter, M.; Burner, H.; Marzinka, S.; Benz, R.; Kasianowicz, J. J. Interaction of poly(ethylene-glycols) with air-water interfaces and lipid monolayers: investigations on surface pressure and surface potential. *Biophys. J.* **1995**, *69*, 1372−1381.

(15) Kojima, M.; Ishihara, K.; Watanabe, A.; Nakabayashi, N. Interaction between phospholipids and biocompatible polymers containing a phosphorylcholine moiety. *Biomaterials* **1991**, *12*, 121−124.

(16) Lee, R. C.; River, L. P.; Pan, F. S.; Ji, L.; Wollmann, R. L. Surfactant-induced sealing of electropermeabilized skeletal muscle membranes in vivo. *Proc. Natl. Acad. Sci. U. S. A.* **1992**, *89*, 4524−4528.

(17) Frim, D. M.; Wright, D. A.; Curry, D. J.; Cromie, W.; Lee, R.; Kang, U. J. The surfactant poloxamer-188 protects against glutamate toxicity in the rat brain. *NeuroReport* **2004**, *15*, 171−174.

(18) Lee, J. M.; Grabb, M. C.; Zipfel, G. J.; Choi, D. W. Brain tissue responses to ischemia. *J. Clin. Invest.* **2000**, *106*, 723−731.

(19) Maskarinec, S. A.; Hannig, J.; Lee, R. C.; Lee, K. Y. C. Direct Observation of Poloxamer 188 Insertion into Lipid Monolayers. *Biophys. J.* **2002**, *82*, 1453−1459.

(20) Wu, G. H.; Khant, H. A.; Chiu, W.; Lee, K. Y. C. Effects of bilayer phases on phospholipid-poloxamer interactions. *Soft Matter* **2009**, *5*, 1496−1503.

(21) van Meer, G.; Voelker, D. R.; Feigenson, G. W. Membrane lipids: where they are and how they behave. *Nat. Rev. Mol. Cell Biol.* **2008**, *9*, 112.

(22) Lundbaek, J. A. Regulation of membrane protein function by lipid bilayer elasticity-a single molecule technology to measure the bilayer properties experienced by an embedded protein. *J. Phys.: Condens. Matter* **2006**, *18*, S1305−1344.

(23) Marks, J. D.; Boriboun, C.; Wang, J. Mitochondrial nitric oxide mediates decreased vulnerability of hippocampal neurons from immature animals to NMDA. *J. Neurosci.* **2005**, *25*, 6561−6575.

(24) Lin, B.; Meron, M.; Gebhardt, J.; Graber, T.; Schlossman, M. L.; Viccaro, P. J. The liquid surface/interface spectrometer at ChemMatCARS synchrotron facility at the Advanced Photon Source. *Phys. B* **2003**, *336*, 75−80.

DOI: 10.1021/acs.biomac.9b00621
Biomacromolecules 2019, 20, 3385−3391